Neutron diffraction measurement of residual stresses in CFC/Cu/CuCrZr joints for nuclear fusion technology

2008 J. Phys.: Condens. Matter 20 104260

(http://iopscience.iop.org/0953-8984/20/10/104260)

J. Phys.: Condens. Matter **20** (2008) 104260 (6pp) doi:10.1088/0953-8984/20/10/104260

Neutron diffraction measurement of residual stresses in CFC/Cu/CuCrZr joints for nuclear fusion technology

F Fiori[1], V Calbucci[1], V Casalegno[2], M Ferraris[2], M Salvo[2], A Giuliani[1], A Manescu[1] and F Rustichelli[1]

[1] Dipartimento di Scienze Applicate ai Sistemi Complessi, Sezione di Scienze Fisiche, Università Politecnica delle Marche, Via Brecce Bianche, I-60131 Ancona, Italy
[2] Politecnico di Torino, Dipartimento di Scienza dei Materiali e Ingegneria Chimica, Corso Duca degli Abruzzi 24, I-10129 Torino, Italy

Received 16 July 2007, in final form 6 December 2007
Published 19 February 2008
Online at stacks.iop.org/JPhysCM/20/104260

Abstract

Residual stresses were experimentally determined in specimens of carbon-fibre composite (CFC) brazed to CuCrZr alloy, using neutron diffraction at the E3 instrument of HMI-BENSC (Berlin). The brazing was obtained by means of a Cu interlayer, one side of which was brazed to the CuCrZr alloy, after the other side was joined to CFC by a proprietary technique. Two different samples were investigated, the first one in the 'as-brazed' condition and the second one after thermal fatigue cycling [heating of samples up to 450 °C followed by a fast cooling (>1 °C s^{-1}) to room temperature in air with water quench; the cycles were repeated 50 times for each sample]. Residual stresses were determined in the three principal directions, in the CFC and in the CuCrZr alloy, as a function of the distance from the interface with the Cu interlayer.

The experimental results for the as-brazed specimen are in agreement with the results of FEM calculations available in the literature, while a relaxation of residual stresses in the thermally fatigued specimen is found to be probably ascribed to the formation of microcracks at the CFC/Cu interface.

(Some figures in this article are in colour only in the electronic version)

1. Introduction

A high heat flux plasma facing component, such as the one proposed for the ITER nuclear fusion reactor divertor, is formed by an armour (CFC) and a heat sink material (copper alloy, CuCrZr ITER grade), which transfers the heat from the armour to the water flowing in the cooling channel of the heat sink. One of the most critical steps in the manufacturing of this component is the joint between CFC and the copper alloy (CuCrZr), as it must withstand cyclic thermal, mechanical and neutron loads to provide an acceptable design lifetime and reliability. In particular, the divertor shall sustain 3000 cycles at 10 MW m^{-2} plus 300 cycles at 20 MW m^{-2}.

The main problem related to the CFC–Cu alloy joints is the large thermal expansion mismatch between the two materials, which generates large residual stresses at the interface during the joining process. These residual stresses can partially relax by the introduction of a very ductile layer of pure copper between the CFC composite and the Cu alloy.

While brazing of CuCrZr to pure Cu is straightforward, joining of CFC to pure Cu is not obvious, as C and Cu are not soluble in the solid state and the wetting angle between molten Cu and CFC is 140°. Some joining methods have been assessed in recent years [1–3]. In our case a new process [4] was used, where the CFC-NB31 composite surface is modified by metals of the VIB group such as Cr, Mo and W, deposited by the slurry technique. Subsequently, a heat treatment initiates the solid-state reaction between the metals and the composite. This method is described in more detail in [4–6].

As stated above, in the CFC/Cu/CuCrZr based component the control (and possibly reduction) of residual stresses is crucial, as they may add to external loads thus reducing the in-service component strength. These residual stresses can be calculated by FEM simulations, but it is quite obvious

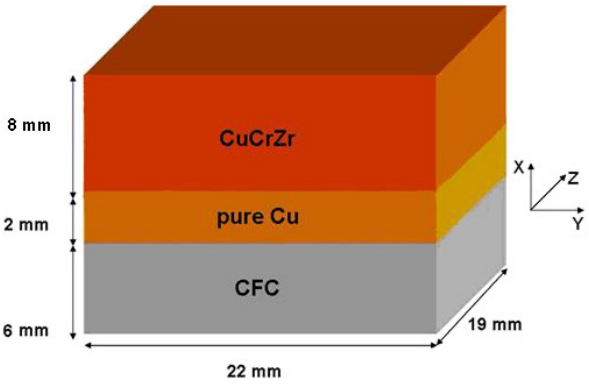

Figure 1. Geometry and reference system of the two investigated samples.

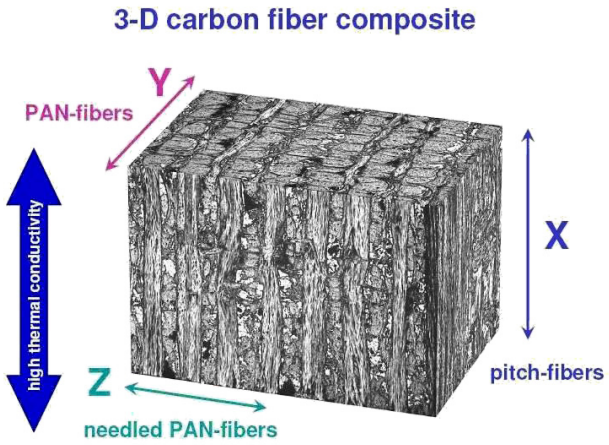

Figure 2. Fibre orientation in CFC-NB31 (courtesy of Dr Linke, Research Centre Juelich, IEF2).

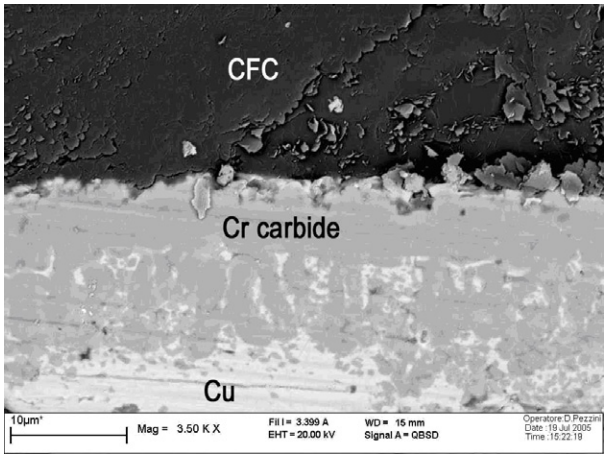

Figure 3. SEM magnification of CFC-NB31/Cr carbide/Cu interface; the total thickness of the carbide layer is about 20 μm.

that an experimental determination, possibly non-destructive, is needed as well.

Some attempts to evaluate residual strains/stresses in brazed structures for fusion technology have been carried out in the past [7, 8] by means of neutron diffraction. The main advantage of this techniques is that it allows investigation of the distribution of the bulk residual stresses along the three principal directions, in a non-destructive way. In principle the contour method could have been used as well, but in this case the specimens would have to be cut in two parts to successively measure the cut surface contour and then evaluate back the 2D residual stress map at the surface (prior to the cut), with the aid of a FEM model. In our case the same specimens had to be submitted to further investigations by other techniques (micro-indentation and mechanical tests), so that only a non-destructive technique such as neutron diffraction could be used.

In this work, this technique is used to determine the residual stress field in a CFC/Cu/CuCrZr assembly, obtained by the procedure described above, both in the 'as-brazed' condition and after thermal fatigue cycling.

2. Materials, specimens and experimental conditions

The geometry of the investigated CFC/Cu/CuCrZr based components is shown in figure 1. The fibre orientation of the CFC is shown in figure 2. The CFC-NB31 surface is modified by depositing a Cr carbide layer, shown in the scanning electron microscopy (SEM) image of the CFC–Cu junction reported in figure 3.

Two different samples were investigated, the first one in the 'as-brazed' condition and the second one after thermal fatigue cycling (50 cycles from room temperature to 450 °C and subsequent quenching in water, as detailed in [4]).

Neutron diffraction experiments were performed at the E3 diffractometer of HMI-BENSC (Berlin), having a fixed neutron wavelength $\lambda = 1.37$ Å, by means of which the Bragg peaks corresponding to reflections (311) for Cu (scattering angle $2\theta \approx 78.06°$) and ($\bar{1}10$) for graphite ($2\theta \approx 67.85°$) could be investigated.

As these peaks are not the most intense ones for both materials, a generally poor scattered intensity was obtained and, as a consequence, too small a sampling volume could not be used. On the other hand, the need to perform a scan along a line parallel to the X direction perpendicular to the joined area surface (figure 3) suggests that the sampling volume should not be too wide in order to get sufficient spatial resolution. Finally, a reasonable compromise was obtained using a $2\times2\times2$ mm^3 volume, determined by 2×2 mm^2 slits on both the incoming and the scattered beam. Nevertheless, with this sampling volume size no statically significant Bragg peak could be obtained from the pure Cu interlayer in a reasonable acquisition time, so that the residual stresses in this part were not measured.

The scan line along X (figure 4) was located in the bulk material, at 4 mm under the surface in both X and Z directions. This choice was made because, using a line through the centre, the neutron path inside the materials would have been too long, thus drastically reducing the diffracted intensity, so that no statistically relevant diffraction peaks could have been recorded during the limited available beamtime.

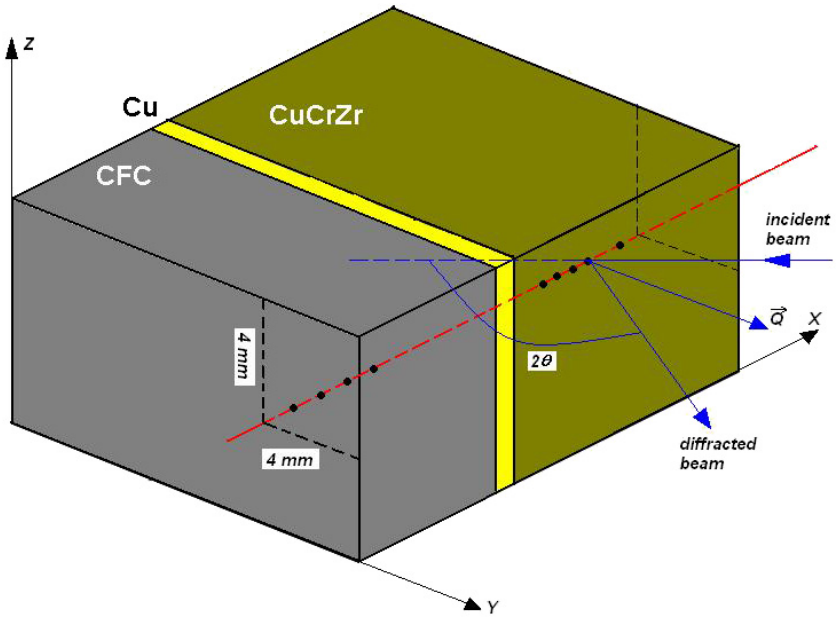

Figure 4. Position of the scan line (for exact positions of the points along X in the CuCrZr alloy and in the CFC, see subsequent figures). An example of strain measurement is also shown: the direction of the exchanged wavevector $\boldsymbol{Q}$ is the one of the measured strain (Y in the figure).

Some preliminary scans were performed in order to choose the optimum depth of the scan line, as it had to be deep enough to avoid edge effects while not keeping the neutron path inside the material for too long. At the same time, due to the plain geometry of the different layers of the specimen, it is reasonable to assume that no dramatic asymmetry effect is expected along a line off the sample central axis like the chosen one.

In each gauge point the three principal strain/stress directions (X, Y and Z) were investigated.

In the CuCrZr alloy the diffraction peak intensities along X, Y and Z strain directions investigated showed no dramatic differences. On this basis, at least in a first approximation, texture was considered to be negligible in CuCrZr.

The unstrained interplanar distance d_0 for CuCrZr was determined in a powder of this alloy. In the CFC, the gauge point the furthest from the Cu layer was assumed to be stress-free, also on the basis that the interplanar distances measured in X, Y and Z directions were coincident within experimental errors. Thus the mean value of them was taken as d_0 for CFC.

3. Data analysis

The 2θ position of the Bragg peak is determined by a Gaussian fit. Using Bragg's law $\lambda = 2d \sin\theta$, the strain can be calculated as:

$$\varepsilon = \frac{d - d_0}{d_0} = \frac{\sin\theta_0}{\sin\theta} - 1 \tag{1}$$

where d_0 is the unstrained interplanar distance of the considered lattice planes, and $2\theta_0$ is the corresponding Bragg peak position.

Finally, the residual stress principal components are obtained using Hooke's law. The Cu alloy can be considered elastically isotropic, so that the stress components can be calculated as follows:

$$\begin{aligned}
\sigma_x &= \frac{E}{(1-2\nu)(1+\nu)}[(1-\nu)\varepsilon_x + \nu(\varepsilon_y + \varepsilon_z)] \\
\sigma_y &= \frac{E}{(1-2\nu)(1+\nu)}[(1-\nu)\varepsilon_y + \nu(\varepsilon_x + \varepsilon_z)] \\
\sigma_z &= \frac{E}{(1-2\nu)(1+\nu)}[(1-\nu)\varepsilon_z + \nu(\varepsilon_x + \varepsilon_y)],
\end{aligned} \tag{2}$$

where E and ν are Young's modulus and Poisson's ratio, respectively. We used the diffractometric elastic constants (DEC) related to the investigated Cu lattice planes (311) [9]:

$$E_{311} = 116\ \text{GPa}; \qquad \nu_{311} = 0.36.$$

Concerning the elastic constants of CFC, the bulk ones were used because they take into account the fibre orientation, unlike the DEC for $(\bar{1}10)$ reflection of graphite. *A posteriori*, this assumption is actually supported by the good agreement of experimental results with FEM for the CFC side of the specimen (see section 4). As CFC is not isotropic, the tensor expression of Hooke's law must be taken into account:

$$\varepsilon_{ij} = S_{ijkl}\sigma_{kl} \tag{3a}$$

or

$$\sigma_{ij} = C_{ijkl}\varepsilon_{kl} \tag{3b}$$

where $\boldsymbol{S}$ and $\boldsymbol{C}$ are the compliance and stiffness tensors, respectively, and $\boldsymbol{C} = \boldsymbol{S}^{-1}$. Anyway, due to their symmetry, the strain and stress tensors can be treated as six-component vectors, and S and C as 6×6 matrices. Moreover, the principal strain (stress) components are independent on the stress (strain)

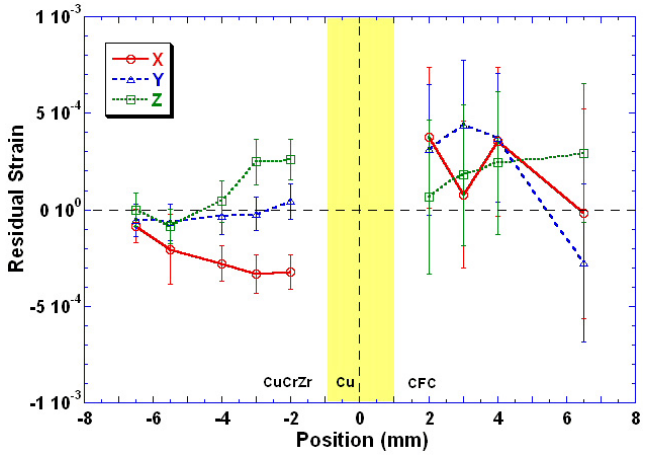

Figure 5. Residual strains in the as-brazed sample (lines are just guides for the eye).

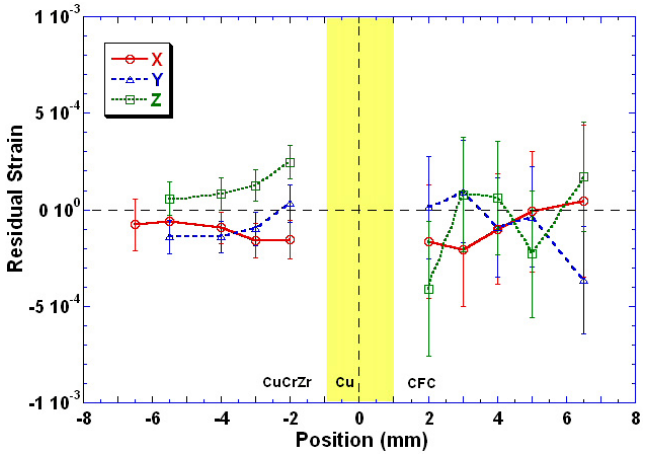

Figure 6. Residual strains in the thermally fatigued sample (lines are just guides for the eye).

Table 1. Elastic constants of CFC-NB31 (at room temperature) [10].

Young's moduli (GPa)	$E_X = 107$	$E_Y = 15$	$E_Z = 12$
Poisson's ratios	$\nu_{XY} = 0.1$	$\nu_{XZ} = 0.2$	$\nu_{YZ} = 0.2$

shear components, and equation (3*a*) can be reduced to

$$\begin{pmatrix} \varepsilon_X \\ \varepsilon_Y \\ \varepsilon_Z \end{pmatrix} = \begin{pmatrix} S_{XX} & S_{XY} & S_{XZ} \\ S_{XY} & S_{YY} & S_{YZ} \\ S_{XZ} & S_{YZ} & S_{ZZ} \end{pmatrix} \begin{pmatrix} \sigma_X \\ \sigma_Y \\ \sigma_Z \end{pmatrix}. \tag{4}$$

The S_{ij} components are related to the values of Young's modulus and Poisson's ratio along the principal directions of the material, and the symmetry of the CFC-NB31 system gives

$$\begin{gathered} S_{XX} = 1/E_X \qquad S_{YY} = 1/E_Y \qquad S_{ZZ} = 1/E_Z \\ S_{XY} = -\nu_{XY}/E_X \qquad S_{YZ} = -\nu_{YZ}/E_Y \\ S_{XZ} = -\nu_{XZ}/E_Z. \end{gathered} \tag{5}$$

The elastic constants for CFC-NB31 are shown in table 1 [10], from which the S_{ij} components are calculated. Finally, inverting the $\boldsymbol{S}$ matrix, the principal components of the stress are obtained by equation (3*b*):

$$\begin{pmatrix} \sigma_X \\ \sigma_Y \\ \sigma_Z \end{pmatrix} = \begin{pmatrix} 172.50 & 9.62 & 36.12 \\ 9.62 & 16.02 & 4.49 \\ 36.12 & 4.49 & 19.96 \end{pmatrix} \begin{pmatrix} \varepsilon_X \\ \varepsilon_Y \\ \varepsilon_Z \end{pmatrix} \tag{6}$$

where the $\boldsymbol{C}$ matrix components are given in GPa.

4. Results and discussion

The measured strains and stresses are shown in figures 5, 6 and 7, 8, respectively, for the as-brazed and the thermally fatigued samples.

In the as-brazed specimen the measured residual stresses are in agreement with expectations and FEM calculation results available in the literature (figure 9, [11]). Due to its higher thermal expansion coefficient with respect to CFC ($\approx 17 \times 10^{-6}$ K^{-1} versus $\approx 1 \times 10^{-6}$ K^{-1}), the CuCrZr alloy would expand more than what is actually allowed by the constraint of the CFC, thus resulting in compression (and the CFC in tension). This residual stress distribution corresponds to the real one, though it is mitigated by plastic deformation of the soft pure Cu compliant layer. Furthermore, being the X direction (perpendicular to the interfaces) in the CFC the one with the maximum value of Young's modulus E (one order of magnitude higher than in other directions—see table 1), the highest thermal stresses developed during the brazing are expected in this direction. This is actually found by neutron diffraction, as shown in figure 7.

As foreseen by FEM (figure 9), in the X direction a compression state is found in the CuCrZr alloy, while tensile stresses are measured in the CFC, and the agreement between calculated and measured stress values in the CFC is satisfactory. Nevertheless, the calculated shape of the residual stress versus position curve is not well reproduced by experimental data in the CuCrZr alloy. This could be ascribed to the different geometry considered (no cooling channel is present in the CuCrZr part of experimentally investigated specimens), different position of the scan (along the element edge in [11], 4 mm under the edge in the experiment), and the eventual presence of texture states in the CuCrZr alloy. Furthermore, it should also be taken into account that experimental values in the different gauge points are actually an average over the sampling volumes ($2 \times 2 \times 2$ mm^3), and that large experimental errors are associated with the measured stresses in the CFC, due to poor scattered intensity in this part. Anyway, each component of the measured residual stresses in the CFC is maintained below the corresponding NB31 tensile strength.

Turning to the thermally fatigued specimen, a general relaxation of residual stresses after the thermal cycling is detected both in the CuCrZr and in the CFC, especially concerning the X component (perpendicular to the joint plane). Indeed, in the CFC the tensile state in the X direction, measured in the as-brazed specimen, is turned into compressive, remaining well below the compressive strength of NB31 along this direction.

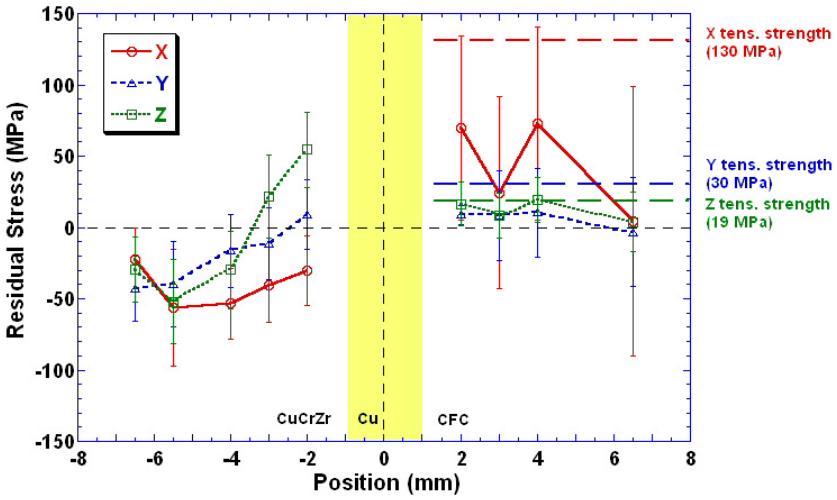

Figure 7. Residual stresses in the as-brazed sample (lines are just guides for the eye). The tensile strengths of CFC-NB31(at room temperature) are also indicated.

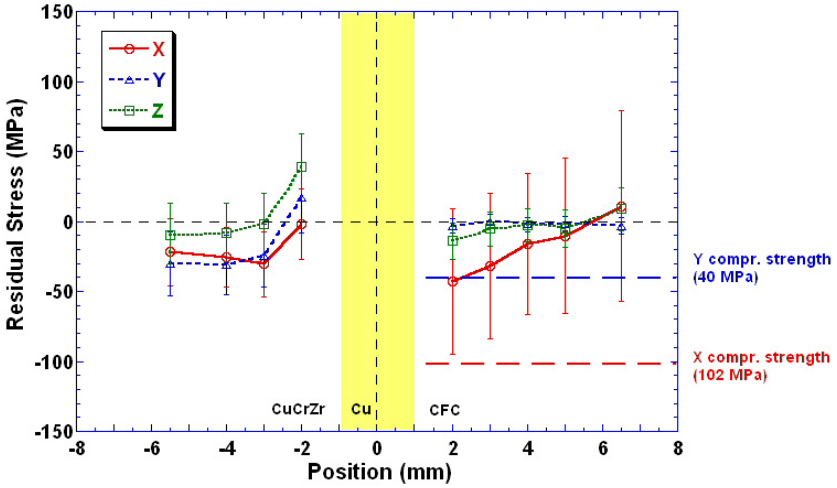

Figure 8. Residual stresses in the thermally fatigued sample (lines are just guides for the eye). The compressive strengths of CFC-NB31 (at room temperature) are also indicated.

Schedler *et al* [12] showed that the CFC–Cu joint strength is weakened after treatments such as quenching and thermal fatigue, due to the formation of microcracks which reduce the integral capability of the joint to transfer mechanical loads. The observed residual stress relaxation could be ascribed to this phenomenon as well. Further morphological analysis will be performed on quenched samples to investigate the presence of defects, i.e. microcracks at the interface, since the CFC–Cu debonding/cracking also can cause the relaxation of the X residual stress in CFC.

The appearance of a compression state in CFC after quenching is not completely understood and will be verified in further experiments with other techniques, such as microindentation. In particular, along the X direction a compressive stress is detected on both CFC and CuCrZr alloy. Actually large stress gradients can be expected in points very close to the CFC–Cu and CuCrZr–Cu interfaces. Therefore, also taking into account that the stress state could not be measured at all in the pure Cu interlayer, it can be expected that tensile residual stresses develop in these regions after the thermal cycling and subsequent quenching, in such a way as to fulfil the overall stress-balance conditions along X.

5. Conclusion

Neutron diffraction was successfully applied to the determination of residual stresses in CFC(NB31)/Cu/CuCrZr based components, with the CFC to pure Cu joining obtained by a new process in which the CFC composite surface is modified by different metals of the VIB group (Cr, Mo, W), deposited by the slurry technique. The results for the as-brazed specimen showed the expected stress states (tensile in the CFC and compressive in the CuCrZr alloy), also in agreement with FEM calculation results available in the literature. The effect of the thermal fatigue cycling was a general relaxation of residual stresses, probably due to the formation of microcracks at the CFC–Cu joint during the cycling.

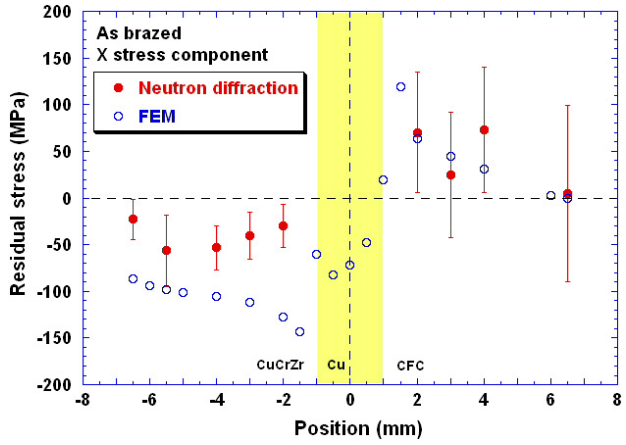

Figure 9. Comparison between measured and calculated residual stresses (*X* component) in the as-brazed sample. The FEM values are extracted from [11].

Acknowledgments

This work was carried out in the framework of the EU Network of Excellence Project 'Knowledge-based Multicomponent Materials for Durable and Safe Performance' (KMM-NoE), contract no. NMP3-CT-2004–502243.

Experiments at HMI-BENSC Berlin were supported by the European Commission under the 6th Framework Programme, Key Action NMI3 'Strengthening the European Research Area, Research Infrastructures', contract no. RII3-CT-2003-505925.

References

[1] Rainer F and Reheis N 1995 Process for the manufacturing of a cooling unit *EP Patent Specification* 0 663 670 (9th January)

[2] Moncel L, Schlosser J, Mitteau R and Plöchl L 1998 Active metal casting technique in plasma facing components: characterisation *Proc. 20th Symp. of Fusion Technology (SOFT) (Marseille, Sept. 1998)* p 133

[3] Merola M, Daenner W, Palmer J, Vieider G and Wu C H 2003 European contribution to the development of the ITER divertor *Fusion Eng. Des.* **66–68** 211

[4] 2004 *Patent* PCT/EP2004/011202 (Politecnico di Torino)

[5] Appendino P, Ferraris M, Casalegno V, Salvo M, Merola M and Grattarola M 2004 Direct joining of CFC to copper *J. Nucl. Mater.* **329–333** 1563

[6] Appendino P, Ferraris M, Casalegno V, Salvo M, Merola M and Grattarola M 2006 Proposal for a new technique to join CFC composites to copper *J. Nucl. Mater.* **348** 102

[7] Ceretti M, Coppola R, Di Pietro E and Nardi C 1998 High-temperature residual strain measurements, using neutron diffraction, in brazed Cu/CFC graphite divertor structures *J. Nucl. Mater.* **258–263** 1005

[8] Albertini G, Ceretti M, Coppola R, Di Pietro E and Lodini A 1996 Neutron diffraction study of internal stresses in brazed divertor structures for ITER *J. Nucl. Mater.* **233–237** 954

[9] Eigenmann B and Macherauch E 1996 Röntgenographische Untersuchung von Spannungszuständen in Werkstoffen *Mat.-wiss. Werkstofftech.* **27** 426

[10] http://www.rijnh.nl/ITER-NL/ITER_FDR/Final%20Design%20Report%20July%202001% 20-% 20Materials% 20Documents/MAR/2PlasmaFacingMaterials/23% 20CFC.pdf FOM Institute for Plasma Physics 'Rijnhuizen', Nieuwegein, The Netherlands

[11] Schlosser J *et al* 2007 CFC/Cu bond damage in actively cooled plasma facing components *Phys. Scr.* T **128** 204

[12] Schedler B *et al* 2007 Methods to determine the joint strength of C/C to copper joints *Fusion Eng. Des* **82** 1786–92